Numerical Study on Forced Convection of Slip Flow in A Microchannel with Smooth and Sinusoidal Walls

Afshin Ahmadi Nadooshan *
Department of Mechanical Engineering,
Shahrekord University, Iran
E-mail: ahmadi@sku.ac.ir
*Corresponding author

Dariush Bahrami
Department of Mechanical Engineering,
Shahrekord University, Iran
E-mail: bahrami.dariush1372@gmail.com

Akram Jahanbakhshi
Department of Mechanical Engineering,
Shahrekord University, Iran
E-mail: a_jahanbakhshi@stu.sku.ac.ir

Received: 24 March 2021, Revised: 16 July 2021, Accepted: 16 July 2021

Abstract: The micro-scale equipment has many advantages, including high thermal performance, high surface-to-volume ratio in heat transfer, small size, low weight, low required fluid and high design flexibility. In this study, fluid flow inside a microchannel is modeled under the assumption of laminar, incompressible, and two-dimensional flow under symmetric boundary conditions. The slip boundary condition is applied to the walls and the flow in the channel output is assumed to be fully developed. The effect of sinusoidal wall with the domain of 0.1 on the hydrodynamic and thermal behavior of the fluid is investigated and the results are compared with the results of smooth wall. The results show that for a constant Reynolds number, the maximum velocity decreases in the microchannel center by increasing the slip coefficient. Also, the comparison between the results of the wavy-wall microchannel and the microchannel with a smooth wall indicates that the heat transfer in the smooth microchannel is less than that in wavy-wall one. Considering the boundary conditions, the thermal behavior of the fluid is approximately the same for two cases in which both walls are sinusoidal and the only upper wall is sinusoidal.

Keywords: Microchannel, Slip Boundary Condition, Slip Flow, Wavy Wall

How to cite this paper: Afshin Ahmadi Nadooshan, Dariush Bahrami, and Akram Jahanbakhshi, "Numerical Study on Forced Convection of Slip Flow in A Microchannel with Smooth and Sinusoidal Walls", Int J of Advanced Design and Manufacturing Technology, Vol. 14/No. 4, 2021, pp. 59-71.
DOI: 10.30495/admt.2021.1926613.1265

Biographical notes: Afshin Ahmadi Nadooshan is Associate Professor of Mechanical Engineering at Shahrekord University, Shahrekord, Iran. He received his PhD in Mechanical Engineering from Isfahan University of Technology, Isfahan, Iran in 2005. His field of research includes Energy efficiency, Turbulence, Two-phase flow, Air conditioning and refrigeration - mechanical installations and heat transfer in microchanneland micro heatsink. **Dariush Bahrami** received his MSc degree in Mechanical Engineering from Shahrekord University in 2020**. Akram Jahanbakhshi** is PhD candidate of Mechanical Engineering at Shahrekord university, Shahrekord, Iran. She received his MSc in Mechanical Engineering from Shahrekord University, Shahrekord, Iran in 2015. Her field of research is study of heat transfer in microchanneland micro heatsink, energy efficiency and nanofluid heat transfer.

1 INTRODUCTION

In recent years, the research on different methods to increase the heat transfer rate has been accelerated. Also, the researchers have been tried to increase convection heat transfer by changing the flow geometry and boundary conditions. In general, heat transfer enhancement techniques can be divided into two active and passive ones. They are as follows, respectively:

A. Active methods:
- Rotating surfaces
- Use of mechanical stirrer
- Oscillation of surfaces
- Generation of an electric field
- Generation of a magnetic field
- Using nanofluid

B: Inactive methods:
- Compression of heat exchangers
- Extended surfaces
- Using microchannels
- Waving the surfaces
- Use of the non-circular ducts
- Increasing the vortical heat transfer

One of the most suitable methods for cooling processors and electronic components is the use of very fine channels called microchannels, which can absorb the heat generated in these parts by passing a fluid through them. The use of a wavy wall due to its widespread use in compact heat exchangers and the aerospace industry, nuclear reactors, aircraft industry, etc. is of interest to researchers and engineers. Due to the low hydraulic diameter, microchannels have great potential for heat absorption. Considering the importance of microchannels in heat transfer, many researchers have investigated fluid flow and heat transfer in these equipment. Thermal performance is one of the important factors in the design of microchannels. In 1981, Tukerman and Peace [1] for the first time studied the fluid flow in microchannels using an array of micro-channels with a nearly rectangular cross-section (height of about 50 to 56 μm and a length of 287 to 320 μm) experimentally. After that, numerous numerical and experimental studies have been performed on this subject. Similar experiments have been carried out by Goldberg [2], Wu and Little [3], Mahalingam [4] and Aminossadati et al. [5]. The gas or liquid fluids flow in micro-channels with the width from 100 to 1000 μm. The main objective in most of these studies is to find the optimal geometry for maximal cooling.

Van Rij et al. [6] numerically investigated the effect of frictional losses and dilution on heat transfer in a rectangular microchannel at constant temperature and constant heat flux. The results of this study showed that the effect of frictional losses, flow work and axial conductivity on the slip flow regime plays an important role for fully developed hydrodynamic and thermal conditions. Karimipour et al. [7] investigated the heat transfer in a microchannel under a constant heat flux for a nanofluid numerically and evaluated the effect of slip and no-slip conditions. Their results indicated that the use of nanofluid increases the heat transfer. Also, the electric field has a significant effect on the heat transfer rate. Jung and Kwak [8] studied a 100-micron hydraulic diameter microchannel experimentally and found that the Nusselt number is a function of Reynolds number and the channel aspect ratio for laminar flow regime.

Jalali and Karimipour [9] studied a microchannel with an injection using alumina/water nanofluid. Their results indicated that heat transfer is significant at high Reynolds number, and an increase in the volume fraction of nanofluid results in an increase in the heat transfer. Mohebbi et al. [10] studied the heat transfer in a channel with extended surfaces containing different nanofluids using the lattice Boltzmann method. They stated that the average Nusselt number increases by increasing the volume fraction of nanofluid from 0 to 5%. Nikkhah et al. [11] studied a microchannel with alternating flux on the channel wall and slip boundary condition on the wall. According to their results, the slip coefficient increases the velocity on the channel wall. Also, at low Reynolds numbers, the slip coefficient has not much effect on the average Nusselt number. Kamali and Binesh [12] studied the forced convection heat transfer of copper oxide/water nanofluid in microchannel under constant heat flux and concluded that the heat transfer coefficient and the Nusselt number increase. By evaluating a constant temperature microchannel, Raisi et al. [13] showed that slip coefficient has no significant effect on heat transfer at low Reynolds numbers, but the heat transfer increases with slip coefficient at high Reynolds numbers.

Nazari et al. [14] experimentally investigated the heat transfer of a constant temperature porous tube. They found that the heat transfer of nanofluid is larger than that of pure water. Arabpour et al. [15] studied a microchannel with slip boundary condition and the existence of a heat source and found that different Reynolds numbers and thermal oscillatory flux significantly affect the Nusselt number, and this effect is more visible for the Reynolds numbers between 10 and 100. Also, the minimum amount of heat transfer decreases significantly by increasing the slip velocity at the slip surface, resulting in an increase in the heat transfer. Kuddusi et al. [16] investigated the effect of constant heat flux and constant temperature in different situations on a three-dimensional channel. In this study, they showed that when a wall along the length of the cross section has constant heat flux and three other walls are adiabatic, the Nusselt number decreases by

increasing the aspect ratio at a constant Knudsen number. If the wall is in line with the width of the channel that has constant heat flux and three other walls are adiabatic, the Nusselt number increases by increasing the aspect ratio at a constant Knudsen number. Esmaeilnejad et al. [17] studied a three-dimensional channel with constant heat flux applied on the wall. They found that as the Reynolds number increases, the pressure drop of fluid in the channel increases. Also, the pressure drop increases with the volume fraction of nanofluid at a constant Reynolds number.

In some studies, roughness on the surfaces has been considered to increase the heat transfer rate compared to micro-channels having smooth surfaces. Toghraie et al. [18] studied the fluid flow and heat transfer in a microchannel with smooth, sinusoidal and zigzag-shaped walls for a nanofluid and pure fluid. In this study, the effects of channel length, the volume fraction and Reynolds number on heat transfer were investigated. The results showed that the Nusselt number increases with the volume fraction of copper oxide nanoparticles. It was also concluded that the use of sinusoidal wall for pure fluid is more effective on heat transfer than using nanoparticles for the case of smooth wall. Karimipour et al. [19] investigated the fluid flow and heat transfer for a silver/water nanofluid in a rectangular two-dimensional microchannel with constant temperature. The calculations were performed for two ranges of Reynolds number. The results showed that the presence of the ribs in the microchannel wall leads to an increase in dimensionless velocity and temperature in the central line of the channel. The heat transfer rate is also affected by the concentration of nanoparticles and the Reynolds number.

Bian et al. [20] studied the characteristics of flow and mass transfer in an axisymmetric sinusoidal tube experimentally. Their results showed that the wavelength and amplitude of the sinusoidal tube affect the characteristics of the fluid flow and mass transfer. Heidari and Kermani [21] investigated the effect of nanoparticles on forced convection heat transfer in a sinusoidal channel. They solved the governing equations by using the control volume method based on the SIMPLE method. Their results showed that the addition of nanoparticles into the base fluid and also the waveforms of the walls considerably increase the heat transfer between the wall and the flow. They found that the density of isotherms increases with the Reynolds number. Solehati et al. [22] proposed a microchannel with a wave structure and argued that the mixing performance in this microchannel is better than that in a straight one due to the presence of alternative secondary flow and turbulent flow regime

Rostami et al. [23] studied a three-dimensional wavy microchannel in the presence of 100 and 150 nm diameter nanoparticles. They found that as the diameter of the nanoparticles increases, the increase in the volume fraction has a greater effect on the Nusselt number. Khadem et al. [24] investigated the heat transfer in a microchannel numerically by considering the temperature and velocity jumps and the roughness of the wall surface. Their results showed that the heat transfer is decreased and the pressure drop is increased by increasing the roughness. Yang et al. [25] studied the effect of different parameters such as nanofluid volume fraction, wavelength and Reynolds number on heat transfer in a two-dimensional microchannel and showed that heat transfer increases by increasing the volume fraction of nanofluid.

Lee and Garimella [26] simulated the heat transfer of a laminar flow in the inlet region of a microcannel with a square cross section under uniform heat flux by using FLUENT software. They revealed that there is a good agreement between the numerical results obtained from numerical modeling and the experimental results of other researchers, and so commercial software can be used for modeling and analyzing the microchannels. McHale and Garimella [27] studied the heat transfer in the thermal input region of a trapezoidal microchannel. In this study, the fluid was studied in a single phase under no-slip walls, laminar flow, three dimensional and fully developed flow conditions using Fluent software. Their results indicated that the Nusselt number decreases along the microchannel. They concluded that higher heat transfer can be achieved by increasing the aspect ratio (equivalent to increasing the channel height). Ji et al. [28] studied the effect of the roughness of microchannel wall on heat transfer numerically and showed that the pressure drop increases by increasing the surface roughness. Also, the average Nusselt number increases or decreases with the surface roughness.

2 PROBLEM STATEMENT

Figure 1 shows the schematic of the problem for a microchannel with the aspect ratio of L/h = 30, where L and h are the length and height of the microchannel, respectively. A slip boundary condition is considered for all walls. The numerical simulation is two-dimensional and the lower and upper walls of the channel are divided into three equal parts. The first part of the upper wall is insulated and two other parts are under a constant flux $q'' = 20000(\frac{w}{m^2})$. Also, the two initial parts of the bottom wall are at constant temperature of 303 K and another part is insulated. The effect of different parameters such as dimensionless no-slip coefficient (β = 0, 0.04, 0.08) and Reynolds number (Re = 10, 50, 100) are investigated. The flow in the microchannel is considered to be laminar and incompressible. At the

microchannel entrance, the water enters at 293 K. In the following, the microchannel is considered with the sinusoidal wall structure and the results are compared at each step. The physical properties of pure water are given in "Table 1".

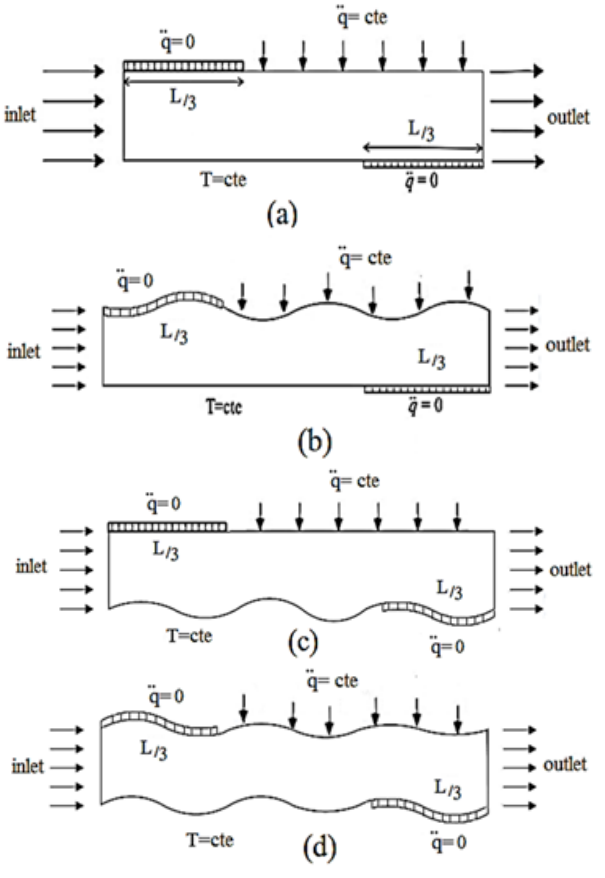

Fig. 1 The schematic of the problem.

Table 1 Properties of water

	Cp($\frac{J}{Kg\,k}$)	)ρ($\frac{kg}{m^3}$	K($\frac{W}{m\,k}$)
Water	4182.0	997.1	0.6

3 GOVERNING EQUATIONS

The flow is assumed to be two-dimensional, steady, incompressible and laminar. Hence, the continuity, momentum, and energy equations that govern the present problem are as follows, respectively:

$$\nabla.\vec{V} = 0 \tag{1}$$

$$\rho\vec{V}.\nabla\vec{V} = -\nabla p + \mu\nabla^2\vec{V} \tag{2}$$

$$\rho C_p\vec{V}.\nabla T = k\nabla^2 T \tag{3}$$

The flow enters the channel at uniform temperature and velocity. The first-order slip boundary condition is used for the walls as follows:

$$\Delta u|_{wall} = L_s\frac{\partial u}{\partial n}\Big|_{wall} \tag{4}$$

Where, u is tangential velocity and n is vertical vector to the wall. L_s (m) is the slip length that is the distance from which the velocity profile becomes zero using extrapolation, in which case the continuity condition is satisfied [29]. As shown in "Fig. 2", the flow velocity is not zero on the wall.

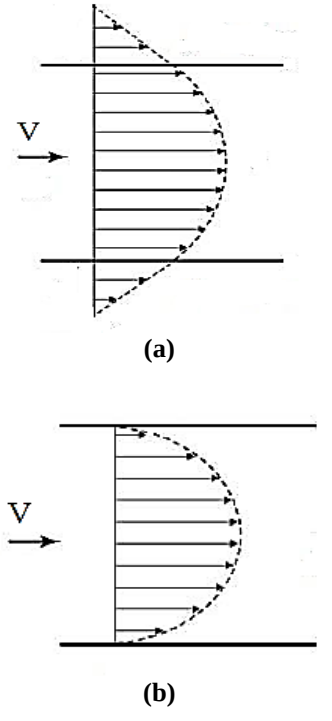

Fig. 2 The comparison of velocity porofile for slip and no-slip flows in a microchannel: (a): The velocity porofile for slip boundary condition, and (b): The velocity porofile for no-slip boundary condition.

The equations are solved using finite element method by using COMSOL software. Relations (5) are used to non-dimensionalize the equations:

$$Y = \frac{y}{h}\ ,X = \frac{x}{L},\ \theta^*_{out} = \frac{T-T_c}{T_h-T_c}\ ,\Theta = \frac{T-T_c}{\Delta T}$$
$$\Delta T = \frac{q_w h}{k}\ ,\quad U = \frac{u}{U_{in}},\ \lambda = \frac{q_w^{"}}{T_s-T_c}$$
$$Nu_{ave} = \frac{1}{L}\int_0^L Nu(x)dx\ ,\ \beta = \frac{L_s}{h}$$
$$Re = \frac{2\rho U_{in}h}{\mu}\quad ,\quad Nu(x) = \frac{\lambda.h}{k[T_s-T_c]} \tag{5}$$

4 GRID STUDY AND VALIDATION

The structural grid is used for the simulations ("Fig. 3"). Since the temperature and velocity gradient is larger in the vicinity of the walls, the boundary mesh is created in these regions. On the other hand, when the fluid passes through the insulated boundary to constant heat flux boundary, a finer grid is created due to the sudden change in the temperature gradient in this area, and also to provide higher accuracy of the simulations.

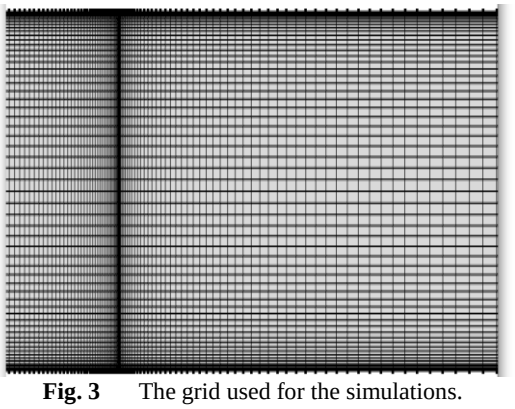

Fig. 3 The grid used for the simulations.

Table 2 shows the average temperature at the microchannel output for different grid resolutions for the boundary condition $\beta = 0.04$, Re = 100, and pure water. According to the results, the change in temperature at the channel outlet is negligible for two grid resolutions of 60×450 and 100×800. Thus, the grid resolution of 60×450 is used for further simulations.

Table 2 Comparison of dimensionless temperature for different grid resolutions.ions

Grid resolution	20×150	40×300	60×450	80×600	100×800
$\theta^*_{ave.out}$	0.237	0.23725	0.23728	0.23727	0.23727

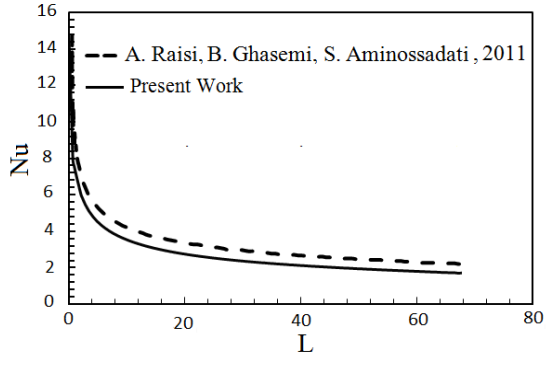

Fig. 4 Comparison between the present results and those reported by Raisi et al. [7].

In order to verify the present method, local Nusselt number obtained from this study is compared with the results of Raisi et al. [7] ("Fig. 4"). This figure demonstrates that the present results are in very good agreement with the results of Raisi et al. [7].

5 RESULTS

5.1. Microchannel with Smooth Walls

Figure 5 shows the velocity profile for Re = 100 and various slip coefficients. As it is shown, with respect to the slip condition ($\beta \neq 0$), the velocity is not zero near the channel walls. It can be seen that the velocity increases in the vicinity of the walls and decreases in the channel center by increasing the slip coefficient. In other words, for a constant Reynolds number, the maximum velocity decreases in the microchannel center with the slip coefficient. In addition, it is clear that the slip coefficient has a significant effect on the velocity profile. Velocity changes between the slip coefficients $\beta = 0$ and $\beta = 0.04$ is larger than that between $\beta = 0.04$ and $\beta = 0.08$. This comparison shows that the difference between the velocity decreases by increasing the slip coefficient. In general, it is clear that the velocity gradient is larger for small dimensions compared to macro dimensions. In the central axis of the microchannel (x-direction), the velocity gradient increases with the slip coefficient.

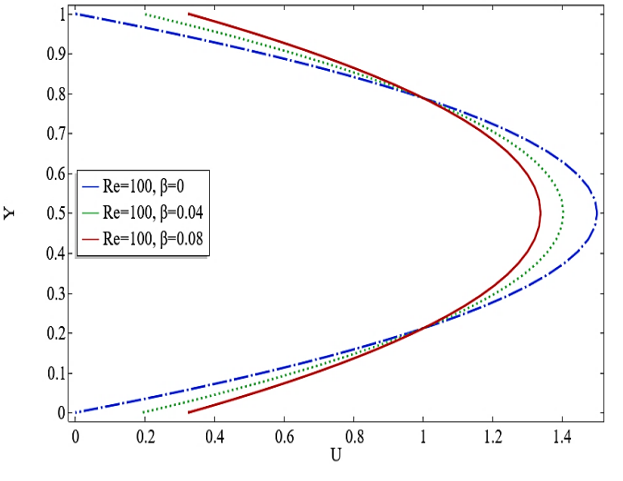

Fig. 5 The velocity profile in the central axis of the microchannel for various slip coefficients**.**

Figure 6 shows the velocity in the vicinity of the microchannel wall (slip velocity ($\beta \neq 0$) and no-slip one ($\beta = 0$)) for $\beta = 0$, 0.04 and 0.08. According to the figure, slip coefficient has a significant effect on slip velocity. The slip velocity starts from its maximum value at the microchannel input, then decreases and ultimately reaches a constant amount along the wall. However, the

range of constant slip velocity along the wall is the same for all slip coefficients. Also, the maximum velocity U_s is obtained for the maximum slip coefficient.

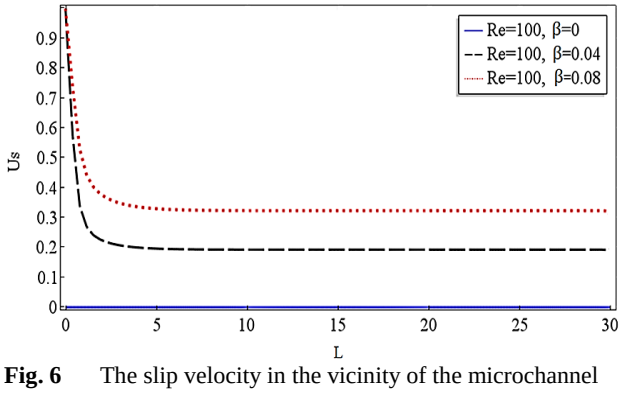

Fig. 6 The slip velocity in the vicinity of the microchannel wall.

Figure 7 shows the local Nusselt number for different Reynolds numbers in a no-slip flow. According to this figure, the heat transfer increases with the Reynolds number. Since the Nusselt number is zero on the insulated wall, the maximum Nusselt number begins from the beginning of the area under the heat flux. It is quite obvious that the Nusselt number on the insulated wall is zero, because there is no heat transfer from these walls. So, the Nusselt number starts from its maximum value and then decreases with a slight slope along the channel, and finally reaches a constant. As the Reynolds number increases, the Nusselt number increases. High Reynolds numbers indicate higher velocities that disturb the flow, resulting in an increase in the heat transfer.

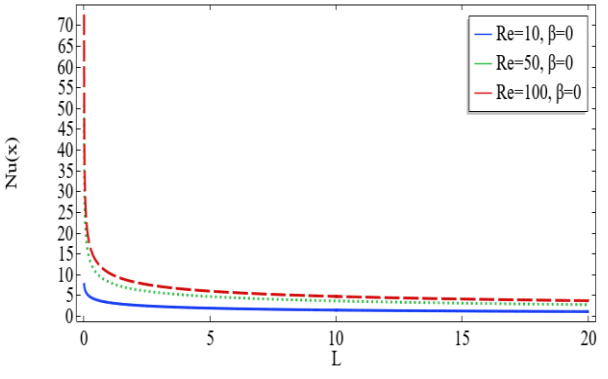

Fig. 7 The local Nusselt number along the channel for different Reynolds numbers.

Figure 8 shows the isothermal lines for Re = 10, 50, 100. It is clear that the density of isothermal lines increases with the Reynolds number. Also, the location of the thermal entrance becomes closer to the channel output by increasing the Reynolds number. Figure 9 shows the temperature variations at the microchannel output for different values of Reynolds number and various slip coefficients. At Re = 10, the fluid temperature rapidly increases due to the low flow velocity. It can be seen that the slip velocity coefficient does not have a significant effect on dimensionless temperature profile, but the effect of slip velocity coefficient on the temperature distribution increases with the Reynolds number.

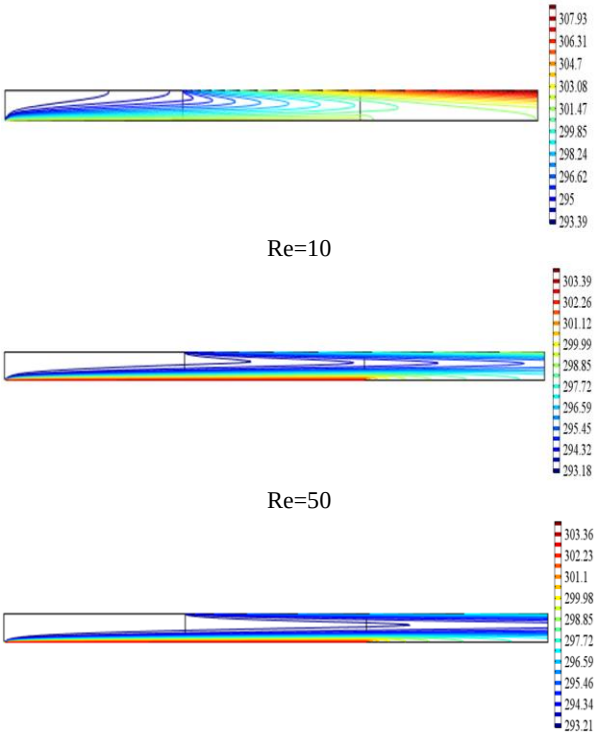

Fig. 8 Isothermal lines along the microchannel.

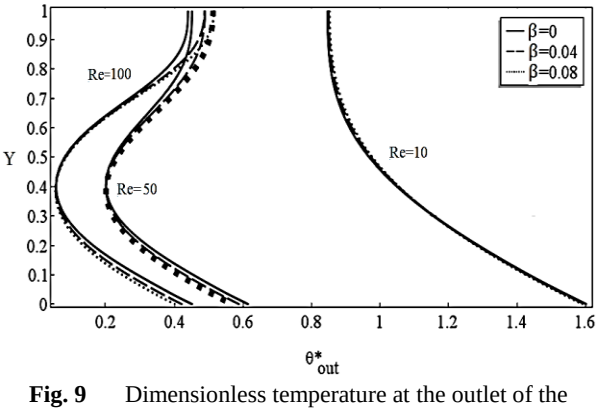

Fig. 9 Dimensionless temperature at the outlet of the microchannel.

Also, it is observed that at the Reynolds numbers of 50 and 100, the temperature profile is almost symmetry relative to the central axis of the channel and has a similar trend for slip and no-slip flows due to the asymmetry of the boundary conditions at the outlet (the

bottom side of the microchannel at the outlet is insulated and the top side is under constant heat flux). It can also be concluded that at low Reynolds numbers, the slip coefficient does not have a significant effect on the thermal behavior of the flow, but at high Reynolds numbers, the heat transfer slightly increases in the vicinity of the top side of the microchannel with increasing the slip coefficient.

In recent years, several methods have been investigated to make industrial equipment more efficient and cost-effective, including the use of microchannels with wavy walls. Today, corrugated channels are widely used in various industries such as aerospace, petrochemicals, petroleum, nuclear industry, etc. to transfer the fluid. In this study, due to the lack of similarity of the boundary conditions applied to the top and bottom walls of the microchannel, each wall is initially considered as sinusoidal one and then both walls are considered as sinusoidal synchronous ones (Y = 0.1 Sin (50×π×X)). The wavy channel operates in a steady incompressible flow. The governing boundary conditions are similar to the microchannel with smooth walls.

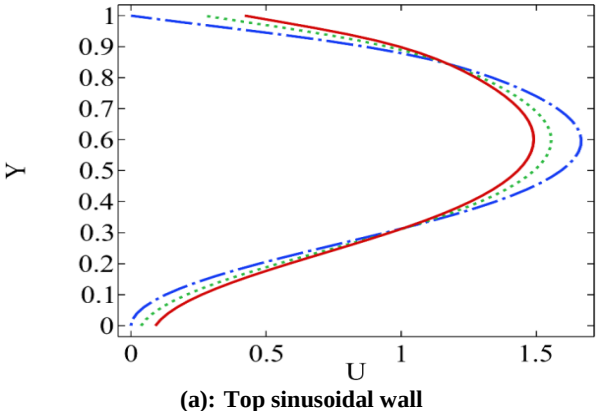

(a): Top sinusoidal wall

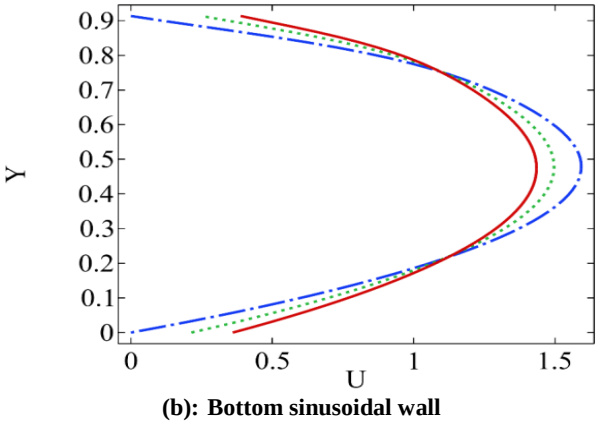

(b): Bottom sinusoidal wall

Fig. 10 The velocity profile along the axial center of the microchannel for different slip coefficients.

Figure 10 shows that the flow velocity increases along the cross-section of the microchannel hence, the maximum velocity occurs at the center of the channel. As far as the central axis of the microchannel is concerned, it seems that the velocity for the case of bottom sinusoidal wall is more than that of top wavy wall. In other words, the slope of the increase in the velocity from the wall to the center of the microchannel is higher for the case (b). Under these conditions, like the smooth-wall microchannel, the maximum velocity in the microchannel center decreases by increasing the slip coefficient for a constant Reynolds number.

In "Fig. 11", the slip velocity on the top wall of the microchannel is compared. It can be seen that for a smooth wall, the slip velocity starts from its maximum value at the microchannel input, then decreases and reaches a constant value on the wall. This variation is observed as oscillating form for the wavy wall.

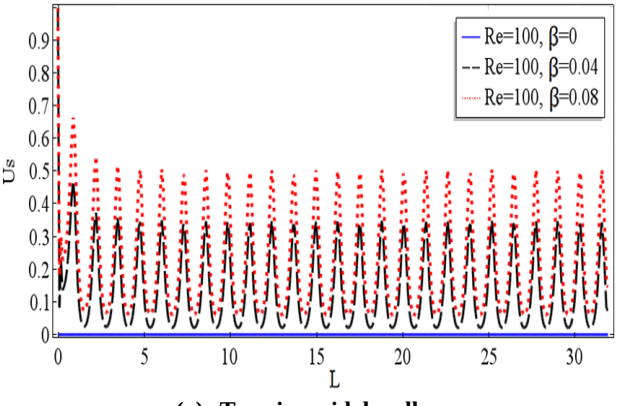

(a): Top sinusoidal wall

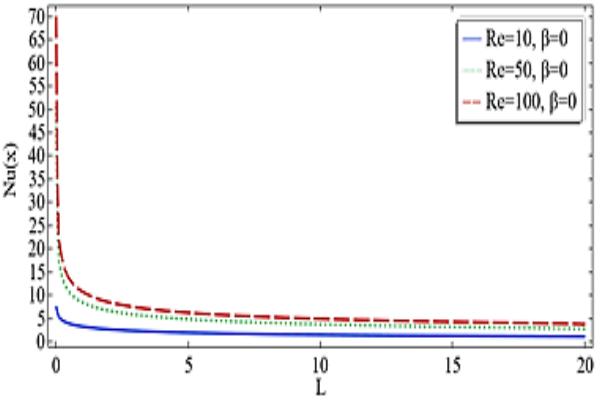

(b): Bottom sinusoidal wall

Fig. 11 The slip velocity on the top wall of the microchannel.

Figure 12 compares the distribution of the Nusselt number for two channels. It can be seen that, the Nusselt numbers decreases and reaches a constant value in fully developed region as the fluid moves in the microchannel. It is shown that the distribution of the oscillation of the Nusselt number is smaller for the wavy wall than that for the smooth wall.

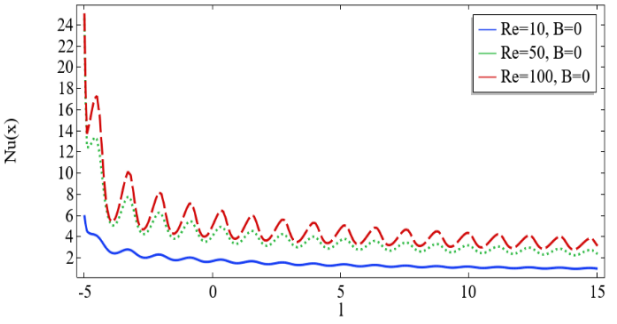

(a): Top sinusoidal wall

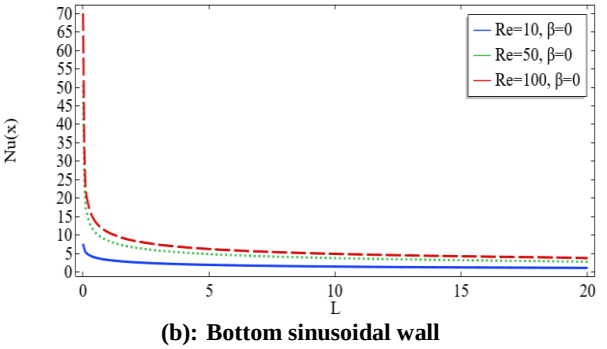

(b): Bottom sinusoidal wall

Fig. 12 The distribution of local Nusselt number in the direction of the top wall for the case of sinusoidal wall.

In this case, it is also clear that the density of isothermal lines in the vicinity of the walls increases with the Reynolds number ("Figs. 13 and 14").

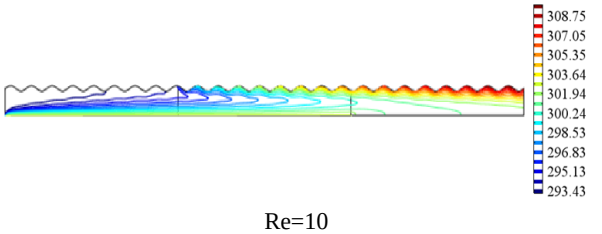

Re=10

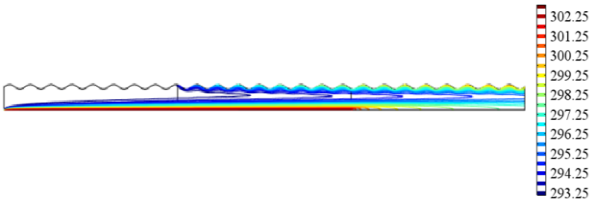

Re=50

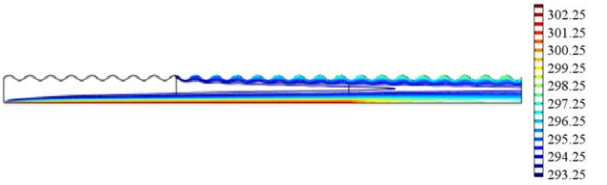

Re=100

(a): Top sinusoidal wall: Re: 10, 50, 100

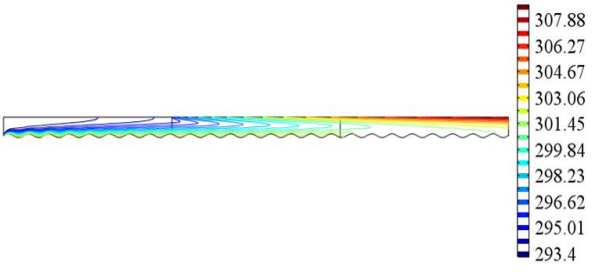

Re=10

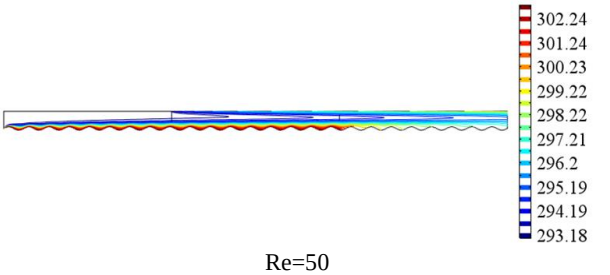

Re=50

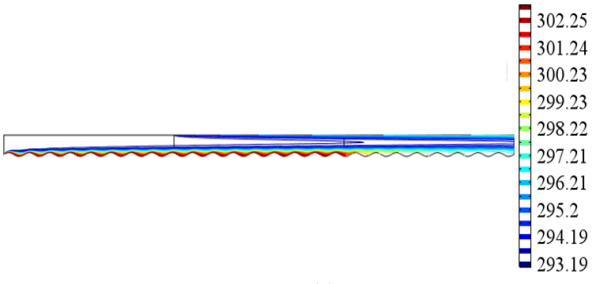

Re=100

(b): Bottom sinusoidal wall: Re: 10, 50, 100

Fig. 13 Isothermal lines for the case of sinusoidal wall.

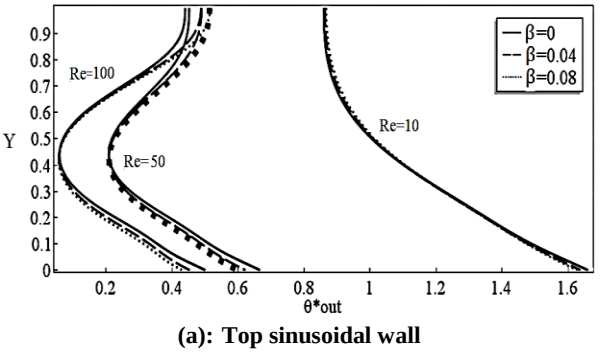

(a): Top sinusoidal wall

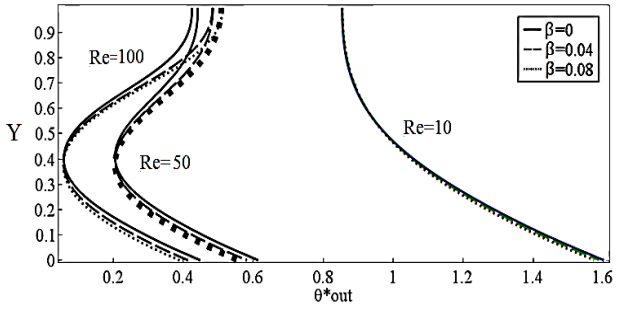

(b): Bottom sinusoidal wall

Fig. 14 Average dimensionless temperature at the output for the case of sinusoidal wall.

5.2. Microchannel with Top and Bottom Sinusoidal Walls

In this section, the microchannel performance with wavy walls with no phase difference and wavelength of 0.1 is investigated. Figure 15 shows the velocity profile in the central axis of the microchannel. It is clear that the velocity changes in the cross sectional surface are similar to those of the top sinusoidal wall of the microchannel. In "Fig. 16", local Nusselt number along the top wall of microchannel is shown.

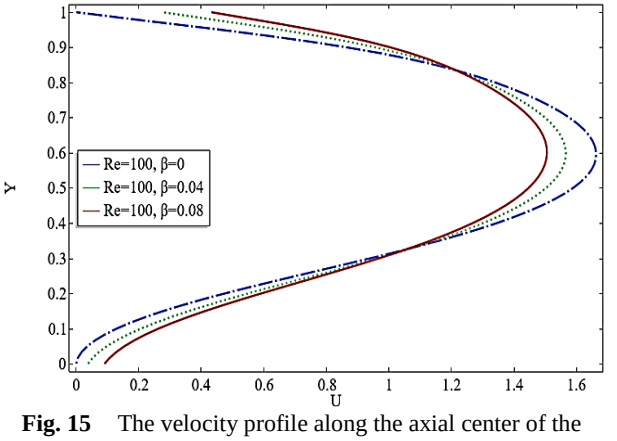

Fig. 15 The velocity profile along the axial center of the microchannel for different slip coefficients.

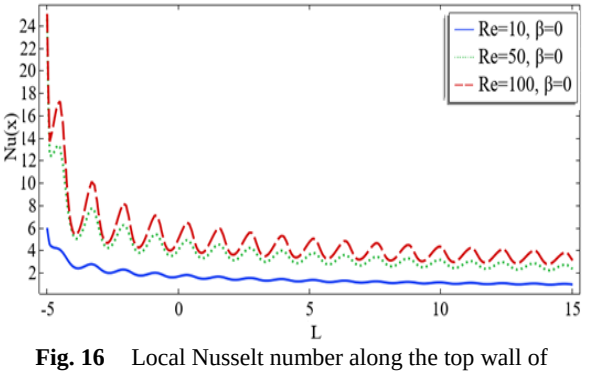

Fig. 16 Local Nusselt number along the top wall of microchannel.

In a microchannel with a sinusoidal wall, the local Nusselt number in the convergent part of the wall is greater than that in the divergent part. The reason is higher velocity gradient in the convergent part that leads to an increase in the heat transfer in these regions. Conversely, the reverse flow near the wall has a low velocity in the divergent part that results in a reduction in the heat transfer rate. For all simulations, an increase in the Reynolds number leads to an increase in the Nusselt number.

In "Fig. 17", slip velocity variations are shown for the top wall of the microchannel. It is clear that higher slip coefficients have a positive effect on slip velocity for all cases. Figure 18 also shows the isothermal lines for the case where both walls are sinusoidal.

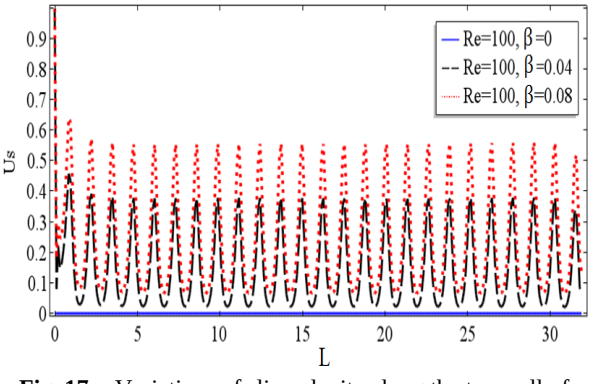

Fig. 17 Variations of slip velocity along the top wall of microchannel.

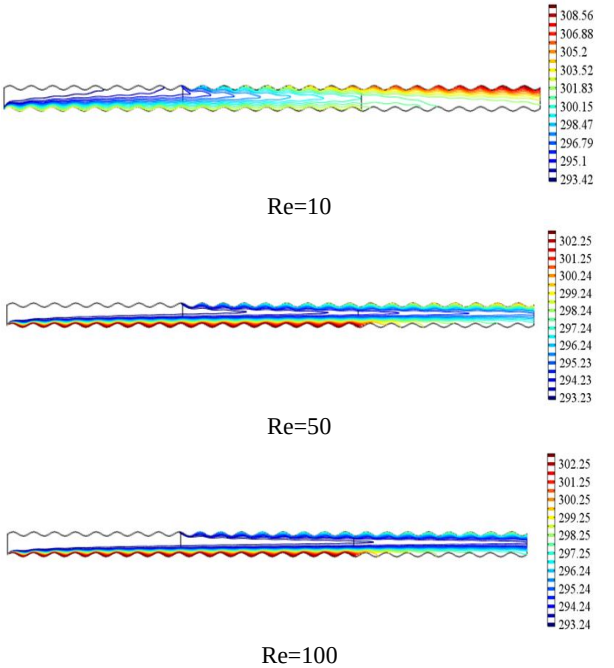

Fig. 18 Isothermal lines along the microchannel.

Figure 19 shows that slip coefficients are more effective on average dimensionless temperature at higher Reynolds numbers.

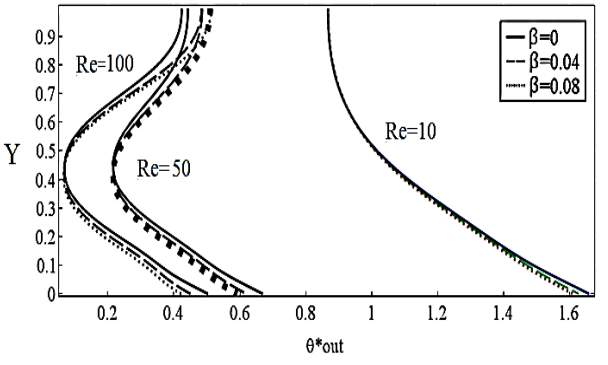

Fig. 19 Average dimensionless temperature at the output of the microchannel.

Figure 20 shows the thermal performance of the microchannel with different wall structures. By comparing the average Nusselt number along the channel for different Reynolds numbers and different slip coefficients, it is observed that the average Nusselt number increases with increasing the Reynolds number for all cases.

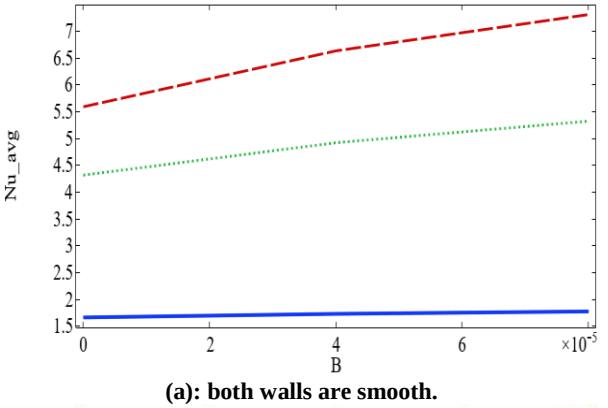

(a): both walls are smooth.

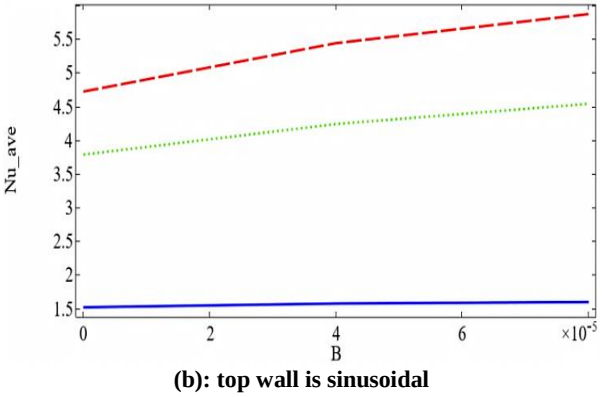

(b): top wall is sinusoidal

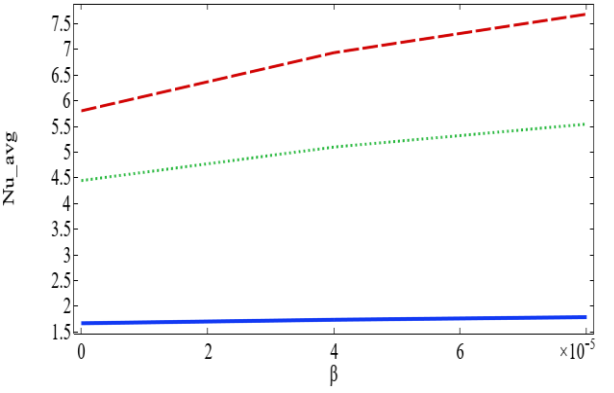

(c): bottom wall is sinusoidal

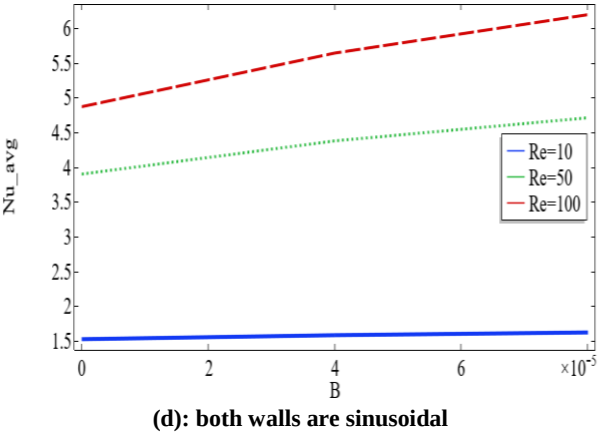

(d): both walls are sinusoidal

Fig. 20 Average Nusselt number for different geometries of the walls of the microchannel.

It is also clear that the fluid thermal behavior in the microchannel is almost identical for a situation in which both walls are sinusoidal and the only top wall is sinusoidal. It is also clear that the effect of slip coefficient β on the increase of Nu_{avg} is more significant with the Reynolds number (Re = 100). Hence, at the Reynolds number of 10, the slip coefficient does not have a significant effect on the thermal performance of the flow.

5.3. Dimensionless Temperature at The Outlet

Table 3 shows the dimensionless temperature at the channel output. By comparing the four microchannel cases, it is observed that in the channel with both sinusoidal walls, the dimensionless temperature at the channel output is higher than other geometries, which indicates that the water absorbs more heat and the heat transfer is greater than other cases for this type of microchannel.

Table 3 Dimensionless temperature (θ*) at the outlet

Re	β	Both walls are smooth	Top wall is sinusoidal	Bottom wall is sinusoidal	Both walls are sinusoidal
	0	1.061730017	1.102011258	1.068547253	1.10759066
10	0.04	1.063968539	1.099357406	1.065193244	1.101116221
	0.08	1.065180085	1.106996167	1.060535018	1.096872112
	0	0.347049193	0.365110669	0.345506758	0.364073307
50	0.04	0.351834888	0.368047055	0.352367488	0.368421116
	0.08	0.354382102	0.370698481	0.355060179	0.370045514
	0	0.233967623	0.246115989	0.232608165	0.246269209
100	0.04	0.237277379	0.249061265	0.241080475	0.252774898
	0.08	0.238412938	0.249969829	0.244364217	0.254817869

After this geometry, the highest dimensionless temperature is related to the geometries of sinusoidal top wall, sinusoidal bottom wall, and smooth walls, respectively. It is found that the dimensionless temperature at the channel output increases by increasing the Reynolds number. In "Table 3", the temperature is also calculated for the slip and no-slip conditions. According to the results, the temperature at the channel output increases with the slip coefficient. Regarding the governing boundary conditions, one can expect the best thermal performance for the microchannel corresponding to the geometries of both sinusoidal walls, sinusoidal top wall, sinusoidal bottom wall, and smooth walls, respectively.

6 CONCLUSION

In this study, the fluid flow and heat transfer in a microchannel with smooth and sinusoidal synchronous walls (Y = 0.1 Sin (50×π×X)) were investigated. Slip velocity is used as a boundary condition on the walls of the microchannel. At first, each wall is initially considered as sinusoidal one and then both walls are considered as sinusoidal synchronous ones. The purpose of this study was to find the optimal geometry for the considered microchannel. Comparison of the performance of wavy-wall and smooth-wall microchannels showed that in general, the heat transfer of the microchannels with the wavy wall is larger. When the slip condition is applied, the velocity along the walls is not zero. As the slip coefficient increases, the maximum velocity in the central axis of the channel decreases. At Re = 10, the slip coefficient does not have much effect on the temperature profile. While at high Reynolds numbers, the slip velocity coefficient is more effective on the temperature profile. The Nusselt numbers decreases and reaches a constant value in fully developed region as the fluid moves in the microchannel. It is shown that the distribution of the oscillation of the Nusselt number is smaller for the wavy wall than that for the smooth wall. It was also observed that the hydrodynamic behavior of the fluid flow in the cross-section of the microchannel is similar for the case of wavy walls and the one where only top wall is wavy. Also, the thermal behavior of the fluid flow in the cross-section of the microchannel is similar for the case of wavy walls and the one where only top wall is wavy. If only the increase in the heat transfer is considered, regarding the governing boundary conditions, one can expect the best thermal performance for the microchannel corresponding to the geometries of both sinusoidal walls, sinusoidal top wall, sinusoidal bottom wall, and smooth walls, respectively. Generally, higher values of dimensionless temperature are obtained for all geometries with a wavy wall relative to the smooth-wall channel. The difference is more noticeable for higher Reynolds numbers.

7 NOMENCLATURE

h	Channel height (m)
x	Cartesian coordinate component along the channel length (m)
y	Cartesian coordinate component along channel width (m)
X	Non-dimensional component of Cartesian coordinates along the channel length
Y	Non-dimensional component of Cartesian coordinates along the channel width
$\vec{V}$	Two-dimensional velocity vector along x- and y-directions (m/s)
u	Tangential component of velocity (m/s)
L_s	Slip length (m)
T	Temperature (k)
ρ	Density (kg/m^3)
λ	Convection heat trasnfer coeffcient ($\frac{W}{m^2K}$)
Θ^*	Non-dimensional temperature
θ^*_{out}	Non-dimensional temperature at the channel output

Re	Reynolds number
Nu	Local Nusselt number
Nu_{ave}	Average Nusselt number
β	Non-dimensional slip length
T_c	Cold temperature of the channel

REFERENCES

[1] Tuckerman, D. B., Pease, R. F. W., High-Performance Heat Sinking for VLSI. IEEE Electron Device Letters, Vol. 2, 1981, pp. 126-129.

[2] Goldberg, N., Narrow Channel Forced Air Heat Sink, Ieee Transactions On Components, Hybrids, and Manufacturing Technology, Vol. 7, No. 1, 1984, pp. 154-159.

[3] Wu, P., Little, W. A., Measurement of the Heat Transfer Characteristics of Gas Flow in Fine Channel Heat Exchangers Used for Microminiature Refrigerators, Cryogenics, Vol. 24, No.8 1984, pp. 415-420.

[4] Mahalingam, M., Thermal Management in Semiconductor Device Packaging, Proceedings of the IEEE, Vol. 73, No. 9, 1985, pp. 1396-1404.

[5] Aminossadati, S. M., Raisi, A., and Ghasemi, B., Effects of Magnetic Field On Nanofluid Forced Convection in A Partially Heated Microchannel, International Journal of Non-Linear Mechanics, Vol. 46, No. 10, 2011, pp. 1373-1382.

[6] Van Rij, J., Ameel, T., and Harman, T., The Effect of Viscous Dissipation and Rarefaction On Rectangular Microchannel Convective Heat Transfer, International Journal of Thermal Sciences, Vol. 48, No. 2, 2009, pp. 271–281.

[7] Karimipour, A., Taghipour, A., and Malvandi, A., Developing the Laminar MHD Forced Convection Flow of Water/FMWNT Carbon Nanotubes in A Microchannel Imposed the Uniform Heat Flux, Journal of Magnetism and Magnetic Materials, Vol. 419, 2016, pp. 420-428.

[8] Jung, J. Y., Kwak, H. Y., Fluid Flow and Heat Transfer in Microchannels with Rectangular Cross Section, Heat and Mass Transfer, Vol. 44, No. 9, 2008, pp. 1041-1049.

[9] Jalali, E., Karimipour, A., Simulation the Effects of Cross-Flow Injection On the Slip Velocity and Temperature Domain of a Nanofluid Flow Inside a Microchannel, International Journal of Numerical Methods for Heat & Fluid Flow, 2019

[10] Mohebbi, R., Rashidi, M. M., Izadi, M., Sidik, N. A. C., and Xian, H. W., Forced Convection of Nanofluids in an Extended Surfaces Channel Using Lattice Boltzmann Method, International Journal of Heat and Mass Transfer, Vol. 117, 2018, pp. 1291-1303.

[11] Nikkhah, Z., Karimipour, A., Safaei, M. R., Forghani-Tehrani, P., Goodarzi, M., Dahari, M., and Wongwises, S., Forced Convective Heat Transfer of Water/Functionalized Multi-Walled Carbon Nanotube Nanofluids in A Microchannel with Oscillating Heat Flux and Slip Boundary Condition, International Communications in Heat and Mass Transfer, Vol. 68, 2015, pp. 69-77.

[12] Kamali, R., Binesh, A. R., Numerical Investigation of Heat Transfer Enhancement Using Carbon Nanotube-Based Non-Newtonian Nanofluids, International Communications in Heat and Mass Transfer, Vol. 37, No. 8, 2010, pp. 1153-1157.

[13] Raisi, A., Ghasemi, B., and Aminossadati, S. M., A Numerical Study On the Forced Convection of Laminar Nanofluid in A Microchannel with Both Slip and No-Slip Conditions. Numerical Heat Transfer, Part A: Applications, Vol. 59, No. 2, 2011, pp. 114-129.

[14] Nazari, M., Ashouri, M., Experimental Investigation of Forced Convection of Nanofluids in A Horizontal Tube Filled with Porous Medium, Modares Mechanical Engineering, Vol. 14, No. 9, 2014, pp. 109-116.

[15] Arabpour, A., Karimipour, A., and Toghraie, D., The Study of Heat Transfers and Laminar Flow of Kerosene/Multi-Walled Carbon Nanotubes (MWCNTs) Nanofluid in The Microchannel Heat Sink with Slip Boundary Condition, Journal of Thermal Analysis and Calorimetry, Vol. 131, No. 2, 2018, pp. 1553-1566.

[16] Kuddusi, L., Prediction of Temperature Distribution and Nusselt Number in Rectangular Microchannels at Wall Slip Condition for All Versions of Constant Wall Temperature, International Journal of Thermal Sciences, Vol. 46, No. 10, 2007, pp. 998-1010.

[17] Esmaeilnejad, A., Aminfar, H., and Neistanak, M. S., Numerical Investigation of Forced Convection Heat Transfer Through Microchannels with Non-Newtonian Nanofluids, International Journal of Thermal Sciences, Vol. 75, 2014, pp. 76-86.

[18] Toghraie, D., Abdollah, M. M. D., Pourfattah, F., Akbari, O. A., and Ruhani, B., Numerical Investigation of Flow and Heat Transfer Characteristics in Smooth, Sinusoidal and Zigzag-Shaped Microchannel with and Without Nanofluid, Journal of Thermal Analysis and Calorimetry, Vol. 131, No. 2, 2018, pp. 1757-1766.

[19] Karimipour, A., Alipour, H., Akbari, O. A., Semiromi, D. T., and Esfe, M. H., Studying the Effect of Indentation On Flow Parameters and Slow Heat Transfer of Water-Silver Nano-Fluid with Varying Volume Fraction in A Rectangular Two-Dimensional Micro Channel, Indian J Sci Technol, Vol. 8, No. 15, 2015, pp. 51707.

[20] Bian, Y., Chen, L., Zhu, J., and Li, C., Effects of Dimensions On the Fluid Flow and Mass Transfer Characteristics in Wavy-Walled Tubes for Steady Flow. Heat and Mass Transfe, Vol. 49, No. 5, 2013, pp. 723-731.

[21] Heidary, H., Kermani, M. J., Effect of Nano-Particles On Forced Convection in Sinusoidal-Wall Channel, International Communications in Heat and Mass Transfer, Vol. 37, No. 10, 2010, pp. 520-1527.

[22] Solehati, N., Bae, J., and Sasmito, A. P., Numerical Investigation of Mixing Performance in Microchannel T-Junction with Wavy Structure, Computers & Fluids, Vol. 96, No. 1, 2014, pp. 10-19.

[23] Rostami, J., Abbassi, A., and Harting, J., Heat Transfer by Nanofluids in Wavy Microchannels, Advanced Powder Technology, Vol. 29, No. 4, 2018, pp. 925-933.

[24] Khadem, M. H., Shams, M., and Hossainpour, S., Numerical Simulation of Roughness Effects On Flow and Heat Transfer in Microchannels at Slip Flow Regime, International Communications in Heat and Mass Transfer, Vol. 36, No. 1, 2009, pp. 69-77.

[25] Yang, Y. T., Wang, Y. H., and Tseng, P. K., Numerical Optimization of Heat Transfer Enhancement in A Wavy Channel Using Nanofluids, International Communications in Heat and Mass Transfer, Vol. 51, 2014, pp. 9-17.

[26] Lee, P. S., Garimella, S. V., Thermally Developing Flow and Heat Transfer in Rectangular Microchannels of Different Aspect Ratios, International Journal of Heat and Mass Transfer, Vol. 49, No. 17-18, 2006, pp. 3060-3067.

[27] McHale, J. P., Garimella, S. V., Heat Transfer in Trapezoidal Microchannels of Various Aspect Ratios, International Journal of Heat and Mass Transfer, Vol. 51, No. 1-3, 2010, pp. 365-375.

[28] Ji, Y., Yuan, K., and Chung, J. N., Numerical Simulation of Wall Roughness On Gaseous Flow and Heat Transfer in A Microchannel, International Journal of Heat and Mass Transfer, Vol. 49, No. 7-8, 2006, pp. 1329-1339.

[29] Wang, C. Y., Brief Review of Exact Solutions for Slip-Flow in Ducts and Channels, Journal of Fluids Engineering, Vol. 134, No. 9, 2012.